DALTON

Bis(carboxylato) complexes of platinum(II). Structural and bonding analysis of $[Pt(O_2CR)_2(L–L)]$ [L–L = $2PPh_3$, $Ph_2PCH_2PPh_2$ or $Fe(C_5H_4PPh_2)_2$; R = Me, CF_3, Pr^i or Ph] †

Agnes L. Tan,[a] Pauline M. N. Low,[b] Zhong-Yuan Zhou,[c] Weiming Zheng,[b] Bo-Mu Wu,[c] Thomas C. W. Mak *,[c] and T. S. Andy Hor *,[b]

[a] *Computational Science Programme, Faculty of Science, National University of Singapore, Kent Ridge 119260, Singapore*
[b] *Department of Chemistry, Faculty of Science, National University of Singapore, Kent Ridge 119260, Singapore*
[c] *Department of Chemistry, The Chinese University of Hong Kong, Shatin, N.T., Hong Kong*

Treatment of $[PtCl_2(L–L)]$ [L–L = $2\ PPh_3$, $Ph_2PCH_2PPh_2$(dppm) or $Fe(C_5H_4PPh_2)_2$(dppf)] with $Ag(O_2CR)$ (R = Me, CF_3, Pr^i or Ph) at room temperature generally gave $[Pt(O_2CR)_2(L–L)]$ in moderate to good yields. The crystal and molecular structures of $[Pt(O_2CMe)_2(dppf)]·H_2O$, $[Pt(O_2CPh)_2(dppf)]·CH_2Cl_2$ and $[Pt(O_2CCF_3)_2(dppm)]$ have been determined by single-crystal X-ray diffractometry. All these complexes show a mononuclear square-planar structure with a chelating diphosphine and two neighbouring (*cis*) carboxylates in a monodentate mode. These structures contrast those of the parent $[Pt_4(\mu\text{-}O_2CMe)_8]$ and its derivative $[Pt_4(en)_4(\mu\text{-}O_2CMe)_4]^{4+}$ (en = ethylenediamine) which are tetrameric, based on octahedral Pt^{II}, and contain bridging acetates and direct Pt–Pt bonds. Fenske–Hall molecular orbital calculations of these structures confirmed the existence of Pt–Pt bonding interactions. The presence of hard and electronegative ligands like en and acetate incurs a deficiency in σ-electron density, compared to virtually filled non-bonding orbitals; the former is alleviated by Pt–Pt bonding. d^8 Complexes with ligands like phosphines possessing both σ-donating and π-accepting qualities appear to favour the usual square-planar geometry.

In complexes, carboxylates most commonly adopt a bridging mode.[1] Chelating and monodentate carboxylates are also well known, although many of the latter type are susceptible to chelation [2] or bridge formation because of the proximity effect and/or high basicity of the pendant oxygen. Complexes with two or more carboxylates can display different bonding modes. However, it is very rare for complexes of neighbouring monodentate carboxylates, *viz.* *cis*-$[M(O_2CR)_2L_n]$, to be isolated as they are easily converted into bridging, chelating and even dissociated forms. One notable exception is $[Pt(O_2CR)_2(PPh_3)_2]$ (R = Me [3] or CF_3 [4]) which are stable and have been prepared by oxidation of $[Pt(PPh_3)_4]$. Although the solid-state structures of these complexes have not been crystallographically identified, there seems no doubt that these species are rare examples of complexes with two monodentate carboxylates.

Two recent reports from Jutand and co-workers [5] attracted our attention. They described a spontaneous and quantitative self-reduction of $[Pd(O_2CMe)_2(PPh_3)_2]$ at room temperature (r.t.) to give $[Pd(PPh_3)]$, $OPPh_3$ and $(MeCO)_2O$. Their findings appeared to substantiate (or contradict?) the earlier reports which described the palladium(II) carboxylates as 'stable indefinitely in air' but 'dissociate and decompose readily in warm solvents'.[6] Jutand's reports not only provide a justification for the established usage of $[Pd(O_2CMe)_2(PPh_3)_2]$ as a source of $[Pd^0(PPh_3)_n]$ (without any added reducing agent) in many C–C coupling reactions,[7] especially Heck's reactions,[8] they could explain why complexes with neighbouring monodentate carboxylates are rare, and the considerable difficulties we experienced recently in preparing some related palladium(II) phosphine carboxylates.[9] Since it is difficult to isolate and structurally characterize these palladium(II) complexes, we decided to carry out a series of X-ray crystallographic work on the established platinum(II) analogues, which model these highly catalytically active palladium(II) species.

There is some confusion in the literature regarding the structures of these complexes: $[Pd(O_2CR)_2(PR_3)_2]$ is generally accepted to be mononuclear with both carboxylates in a monodentate mode while $[\{Pd(O_2CR)_2(PR_3)\}_2]$ [10] is dinuclear with bridging and monodentate carboxylates. The former was earlier reported to be a *trans* complex [6] but more recent reports appeared to suggest a *cis* configuration.[11] Both *cis* and *trans* products appear to be isolated from the same reaction.[12] Jutand's reports also assumed a *trans* geometry. The complex $[Pt(O_2CMe)_2(PPh_3)_2]$ [13] is reported to be 'probably *cis*' [14] but the CF_3CO_2 analogue is, strangely, reported to be *trans*.[15] Adding further to this confusion, the structure of the parent $[Pt(O_2CMe)_2]$ was found to be tetranuclear with bridging acetates.[16] It is hence best represented as $[Pt_4(\mu\text{-}O_2CMe)_8]$. The octahedral geometry about d^8-Pt^{II} with Pt–Pt bonds is surprising and, to our knowledge, unexplained. More recently, its ethylenediamine (en) derivative $[Pt_4(en)_4(\mu\text{-}O_2CMe)_4]^{4+}$ was also found to have a similar structure with Pt–Pt bonds and bridging acetates.[17] The assumption that complexes $[Pt(O_2CR)_2(L–L)]$ (L–L = bidentate neutral ligand) are mononuclear with chelating L–L and monodentate carboxylate therefore needs verification. In this paper, we describe the structural and bonding properties of such complexes and compare them with the unusual acetate structures in the literature through X-ray crystallography and Fenske–Hall molecular orbital calculations.

Another objective of this work is to examine if the use of a diphosphine [*e.g.* bis(diphenylphosphino)methane (dppm)] would give isostructural products. In other words, would a diphosphine adopt a bridging mode and hence force changes in the carboxylate bonding mode. It is also uncertain whether two

† *Supplementary data available* 1 (No.SUP 57136, 9 pp.): tables of platinum orbital coefficients and overlap populations matrices.
Non-SI unit employed: eV ≈ 1.60×10^{-19} J.

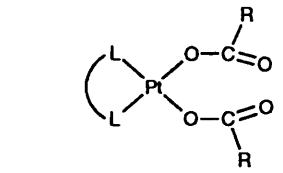

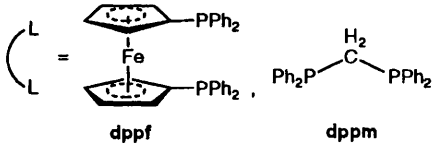

R = Me, CF_3, Pr^i or Ph

diphosphines having very different bites such as dppm and dppf would give isostructural products. The importance of this study is traced to the first report which described a significantly higher activity in Grignard coupling when [$PdCl_2$(dppf)] [dppf = 1,1′-bis(diphenylphosphino)ferrocene] was used as the catalyst compared to its PPh_3 counterpart.[18] Since then, there have been many reports on the advantages associated with the use of dppf in catalytic mixtures.[19] Recent work on Cu^I[20] and Ag^I[21] has suggested a variety of phosphine and carboxylate co-ordination modes which are hard to predict based on solution data.

Results and Discussion

To our knowledge, the only reported dppf or dppm complex of platinum(II) carboxylates [$Pt(O_2CCF_3)_2$(dppm)].[22] For PPh_3, three complexes *viz.* [$Pt(O_2CR)_2(PPh_3)_2$] (R = Me, CF_3 or Ph)[23] have been prepared from [$Pt(PPh_3)_n$] (n = 3 or 4). Treatment of [$PtCl_2$(L–L)] (L–L = 2 PPh_3, dppm, or dppf with Ag(O_2CR) (R = Me, CF_3, Pr^i or Ph) at r.t. generally gave [$Pt(O_2CR)_2$(L–L)] in moderate to good yields. Similar preparations using metathesis have been reported.[24] We preferred this to the more established method which uses Pt^0(L–L)$_2$ as the precursor because of the inconvenience of going through an air-sensitive platinum(0) species, especially the likes of [Pt_2(dppm)$_3$][25] and [Pt(dppf)$_2$].[26] This method is also more direct compared to the use of [$Pt(CO_3)(PPh_3)_2$] (with $MeCO_2H$) as precursor. An early attempt at synthesis of phosphine carboxylate complexes from [$Pt(O_2CMe)_2$] appeared to be unsuccessful.[6] All the present complexes were characterized by IR and ^{1}H and ^{31}P NMR spectroscopy. The large separation ($\delta\nu \approx 250$ cm^{-1}) between the ν_{asym} and ν_{sym} bands is usually a diagnostic feature of a carboxylate ligand in a monodentate mode.[12] The complexes synthesized generally show this feature. Although the co-ordination mode of dppf cannot be ascertained from the NMR data, the ^{31}P shifts of the present series of carboxylates for each particular phosphine generally lie within a narrow window of *ca.* 2 ppm. This is indicative of the isostructural nature of the complexes in solution. The large high-field shift of δ(P) in the dppm complexes is diagnostic of chelating dppm.[24]

In order to establish the structures and bonding properties of these complexes in the solid state we have carried out single-crystal X-ray crystallographic analysis of three representatives, *viz.* [$Pt(O_2CMe)_2$(dppf)] (Fig. 1), [$Pt(O_2CPh)_2$(dppf)] (Fig. 2) and [$Pt(O_2CCF_3)_2(\eta^2$-dppm)] (Fig. 3).* All three complexes show a square-planar Pt^{II} with two carboxylates *cis* to each other. Selected bond lengths and angles are listed in Table 1.

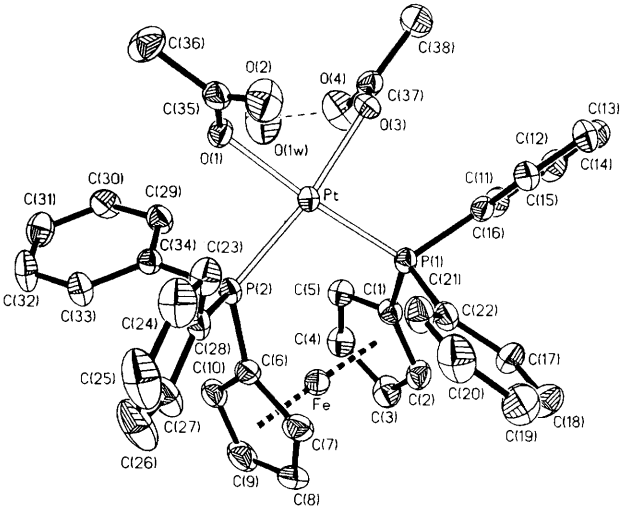

Fig. 1 An ORTEP[27] plot of the molecular structure of [$Pt(O_2CMe)_2$(dppf)]·H_2O with ellipsoids drawn at the 35% probability level (hydrogen atoms omitted for clarity)

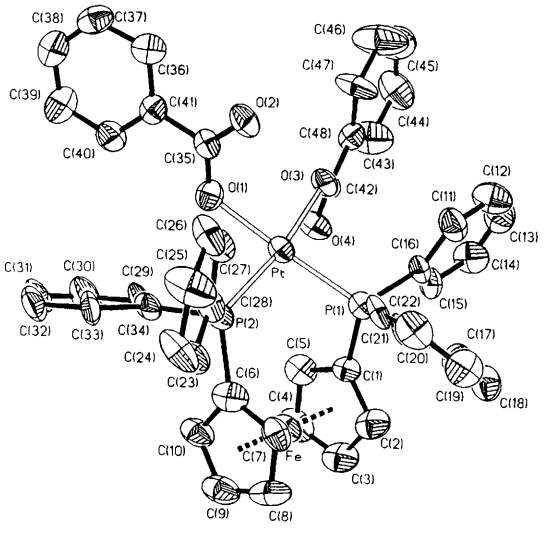

Fig. 2 An ORTEP plot of the molecular diagram of [$Pt(O_2CPh)_2$(dppf)]·CH_2Cl_2 with ellipsoids drawn at the 35% probability level (solvate removed for clarity)

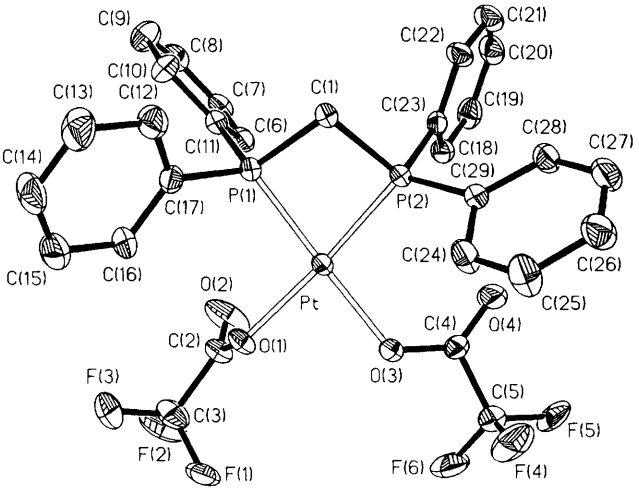

Fig. 3 An ORTEP plot of the molecular diagram of [$Pt(O_2CCF_3)_2$(dppm)] with ellipsoids drawn at the 35% probability level

* Unless otherwise stated, the carboxylate in [$Pt(O_2CR)_2$(L–L)] is monodentate whilst the phosphine is *P,P′* bonded.

Table 1 Selected bond distances (Å) and angles (°)

(*a*) $[Pt(O_2CMe)_2(dppf)]\cdot H_2O$

Pt–P(1)	2.242(1)	Pt–P(2)	2.259(1)	P(2)–C(34)	1.831(4)	C(35)–O(1)	1.298(5)
Pt–O(1)	2.079(3)	Pt–O(3)	2.073(3)	C(35)–O(2)	1.221(6)	C(35)–C(36)	1.502(7)
Fe–C(1–5)	2.039(4)(mean)	Fe–C(6–10)	2.036(4)(mean)	C(37)–O(3)	1.286(5)	C(37)–O(4)	1.210(5)
P(1)–C(1)	1.788(4)	P(1)–C(16)	1.836(4)	C(37)–C(38)	1.515(6)	O(1w) · · · O(2a)	2.916(6)
P(1)–C(22)	1.820(4)	P(2)–C(28)	1.827(4)	O(1w) · · · O(4)	2.836(6)		
P(1)–Pt–P(2)	97.9(1)	P(1)–Pt–O(1)	175.8(1)	Pt–O(3)–C(37)	116.4(2)	O(3)–C(37)–O(4)	124.5(4)
P(2)–Pt–O(1)	86.3(1)	P(1)–Pt–O(3)	89.7(1)	O(3)–C(37)–C(38)	112.5(4)	O(4)–C(37)–C(38)	123.0(4)
P(2)–Pt–(3)	171.9(1)	O(1)–Pt–O(3)	86.1(1)	C(1)–P(1)–C(16)	102.8(2)	C(1)–P(1)–C(22)	109.2(2)
Pt–P(1)–C(1)	114.5(1)	Pt–P(1)–C(16)	115.5(1)	C(16)–P(1)–C(22)	101.2(2)	C(6)–P(2)–C(28)	101.9(2)
Pt–P(1)–C(22)	112.4(1)	Pt–P(2)–C(6)	122.3(1)	C(6)–P(2)–C(34)	100.9(2)	C(28)–P(2)–C(34)	107.2(2)
Pt–P(2)–C(28)	116.4(1)	Pt–P(2)–C(34)	106.3(1)	P(1)–C(1)–C(2)	131.0(3)	P(1)–C(1)–C(5)	122.0(3)
Pt–O(1)–C(35)	119.7(3)	O(1)–C(35)–O(2)	124.2(4)	P(2)–C(6)–C(7)	128.2(3)	P(2)–C(6)–C(10)	126.3(3)
O(1)–C(35)–C(36)	114.2(4)	O(2)–C(35)–C(36)	121.6(4)	O(4) · · · O(1w) · · · O(2a)	138.6(5)		

(*b*) $[Pt(O_2CPh)_2(dppf)]\cdot CH_2Cl_2$

Pt–P(1)	2.219(3)	Pt–P(2)	2.262(3)	P(2)–C(28)	1.79(1)	P(2)–C(34)	1.756(8)
Pt–O(1)	2.034(6)	Pt–O(3)	2.089(6)	C(35)–O(1)	1.28(1)	C(35)–O(2)	1.23(1)
Fe–C(1–5)	2.04(1)(mean)	Fe–C(6–10)	2.05(1)(mean)	C(42)–O(3)	1.28(1)	C(42)–O(4)	1.24(1)
P(1)–C(1)	1.802(9)	P(1)–C(16)	1.850(9)	C(35)–C(41)	1.518(9)	C(42)–C(48)	1.46(1)
P(1)–C(22)	1.807(8)	P(2)–C(6)	1.844(7)	C(49)–Cl(1)	1.71(1)	C(49)–Cl(2)	1.694(9)
P(1)–Pt–P(2)	98.1(1)	P(1)–Pt–O(1)	173.8(2)	O(1)–C(35)–O(2)	127.0(7)	O(1)–C(35)–C(41)	113.2(7)
P(1)–Pt–O(3)	90.6(2)	P(2)–Pt–O(1)	86.4(2)	O(2)–C(35)–C(41)	119.9(7)	C(35)–C(41)–C(36)	119.1(7)
P(2)–Pt–O(3)	171.3(2)	O(1)–Pt–O(3)	84.9(2)	C(35)–C(41)–C(40)	120.3(7)	O(3)–C(42)–O(4)	123.5(8)
Pt–P(1)–C(1)	113.4(3)	Pt–P(1)–C(16)	113.2(2)	O(3)–C(42)–C(48)	115.2(7)	O(4)–C(42)–C(48)	121.2(9)
Pt–P(1)–C(22)	115.4(3)	Pt–P(2)–C(6)	122.8(4)	C(1)–P(1)–C(16)	105.1(4)	C(1)–P(1)–C(22)	106.2(3)
Pt–P(2)–C(28)	113.8(3)	Pt–P(2)–C(34)	108.5(3)	C(16)–P(1)–C(22)	102.4(4)	C(6)–P(2)–C(28)	103.7(4)
Pt–O(1)–C(35)	123.9(5)	Pt–O(3)–C(42)	120.2(5)	C(6)–P(2)–C(34)	101.2(4)	C(28)–P(2)–C(34)	104.8(5)
P(1)–C(1)–C(2)	130.8(7)	P(1)–C(1)–C(5)	120.9(5)				

(*c*) $[Pt(O_2CCF_3)_2(dppm)]$

Pt–P(1)	2.222(2)	Pt–P(2)	2.211(2)	C(4)–O(3)	1.260(9)	C(4)–O(4)	1.191(9)
Pt–O(1)	2.080(4)	Pt–O(3)	2.074(4)	C(4)–C(5)	1.509(8)	C(5)–F(4–6)	1.34(1)(mean)
C(1)–P(1)	1.822(6)	C(1)–P(2)	1.874(6)	P(1)–C(11)	1.804(6)	P(1)–C(17)	1.791(7)
C(2)–O(1)	1.257(8)	C(2)–O(2)	1.195(9)	P(2)–C(23)	1.813(6)	P(2)–C(29)	1.810(6)
C(2)–C(3)	1.509(9)	C(3)–F(1–3)	1.352(9)(mean)				
P(1)–Pt–P(2)	74.1(1)	P(1)–Pt–O(1)	100.0(1)	C(4)–C(5)–F(4–6)	110.9(6)(mean)	Pt–P(1)–C(1)	95.3(2)
P(1)–Pt–O(3)	174.2(1)	P(2)–Pt–O(1)	171.4(1)	Pt–P(1)–C(11)	115.5(2)	Pt–P(1)–C(17)	119.8(2)
P(2)–Pt–O(3)	102.9(1)	O(1)–Pt–O(3)	82.4(2)	Pt–P(2)–C(1)	94.2(2)	Pt–P(2)–C(23)	119.8(2)
P(1)–C(1)–P(2)	92.6(3)	Pt–O(1)–C(2)	122.0(4)	Pt–P(2)–C(29)	117.1(2)	C(1)–P(1)–C(11)	110.1(3)
Pt–O(3)–C(4)	127.3(4)	O(1)–C(2)–O(2)	129.4(7)	C(1)–P(1)–C(17)	108.4(3)	C(11)–P(1)–C(17)	106.8(3)
O(1)–C(2)–C(3)	112.6(6)	O(2)–C(2)–C(3)	118.0(6)	C(1)–P(2)–C(23)	105.5(3)	C(1)–P(2)–C(29)	108.6(3)
O(3)–C(4)–O(4)	129.5(6)	O(3)–C(4)–C(5)	113.8(6)	C(23)–P(2)–C(29)	109.3(3)		
O(4)–C(4)–C(5)	116.7(6)	C(2)–C(3)–F(1–3)	112.1(6)(mean)				

For four-co-ordinate Pt^{II} a chelating phosphine would necessarily force the carboxylates to adopt a monodentate mode. The pendant oxygens are approximately *anti* to each other to avoid non-bonding interactions. These oxygens in the acetate complex are, however, hydrogen bonded to a lattice hydrate. A constitutional isomer of this complex [Pt{C(O)OMe}$_2$(dppf)] with a methoxycarbonyl group, has recently been structurally characterized.[28] Its structure is similar to that of the acetate complex, except that the Pt–P bonds are significantly weaker [2.310(5) and 2.331(5) Å in the methoxycarbonyl complex] which is indicative of the stronger *trans* influence of the C-bonded methoxycarbonyl ligand compared to the O-bonded acetate. Surprisingly, the carboxylates converge at a larger angle (O–Pt–O) for the smaller acetate [86.1(1)°] than benzoate [84.9(2)°]. This is probably reflective of a slight expansion of the acetates in order to accommodate the hydrate. The minimum influence of the carboxylates exerted on the co-ordination angles at the Pt is also reflected in the near-identical chelate angles of dppf in both complexes [97.9(1) and 98.1(1)°]. The chelate angles are typical among the chelating dppf complexes of Pt^{II}.[29] Although it is in general difficult to predict the ferrocenyl ring conformation of dppf in its complexes, we have recently pointed out that a *gauche* (staggered) conformation between the two C_5 rings is the commonest trend for square-planar complexes such as those of Pt^{II} and Pd^{II}.[30] The torsional angles τ* found in the acetate (32.4°) and benzoate (31.6°) complexes are also in agreement with the literature trend. This emphasizes that conformations close to the ideal *gauche* form (τ 36°) are found for planar complexes of Pt^{II}.

The benzoate complex is in general more distorted compared to the acetate and trifluoroacetate complexes. This is best seen by comparing the differences in the Pt–P and Pt–O bonds in the two complexes (Table 1). While the Pt–P bonds in the acetate [δ(Pt–P) 0.017(1) Å] and those of the trifluoroacetate [0.011(2) Å] complexes are similar and the Pt–O [0.006(3) and 0.006(4) Å] virtually identical, the corresponding bonds in the benzoate complex [δ(Pt–P) 0.043(3) and (Pt–O) 0.055(6) Å] are clearly different from each other. The deviations of the co-ordinating atoms from the platinum planes are also more obvious in the benzoate complex. −0.027 to +0.026 Å for the acetate but significantly greater, −0.035 to +0.051 Å, in the benzoate complex. The deviations of the phosphorus atoms from the C_5 planes are also larger for the benzoate (0.097, 0.169 Å) compared to the acetate (0.017, 0.079 Å) complex. These probably originate from the higher interligand repulsions in the benzoate complex.

* Defined as P(1)–X(1)–X(2)–P(2) where X(1) and X(2) are the centroids of the C_5 rings C(1)–C(5) and C(6)–C(10) respectively.

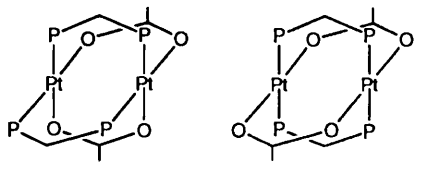

I

II

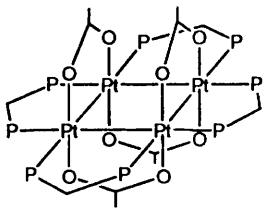

III

Although trifluoroacetate is known to be a weaker ligand compared to acetate, the Pt–O bonds in $[Pt(O_2CCF_3)_2(dppm)]$ [mean 2.077(4) Å] and $[Pt(O_2CMe)_2(dppf)]$ [mean 2.076(3) Å] are identical. The C–O bonds of the former [mean C–O 1.259(8), C=O 1.193(9) Å] however, are significantly stronger than those in the latter [1.292(5) and 1.216(6) Å].

An obvious contrast between the dppm and dppf structures is the bite angle (P–Pt–P) differences of the phosphines [74.1(1)° in the dppm complex and 97.9(1) and 98.1(1)° in the dppf complexes]. The acute bite angle of dppm falls short of the ideal 90° favoured by Pt^{II}. The strain imposed on a four-membered dppm chelate is also reflected in the internal angle at phosphorus [mean C–P–Pt 94.8(2)°] which is substantially less than 109°. A natural question follows: why doesn't dppm open up and convert from a chelating mode into its favoured bridging mode, and as a result the carboxylate could also take up its most favoured bridging position? This ligand rearrangement would result in either a dimeric, **I** or **II**, or tetrameric (**III**) structure. Note that, in these structures, half of the carboxylates are dissociated, which is well known especially for the weakly co-ordinating $CF_3CO_2^-$. Alternatively, all the carboxylates can stay on the metal core as monodentate ligands. Structure **III** would resemble that of $[Pt_4(\mu\text{-}O_2CMe)_8]$ and $[Pt_4(en)_4(\mu\text{-}O_2CMe)_4]^{4+}$ in that the in-plane ligands (O_2CMe or en) are replaced by dppm. This possibility will be addressed below in a molecular orbital (MO) study.

To summarize, the geometric differences of the dppm and dppf chelate rings, although significant, are not sufficiently large to impart any structural changes on these complexes. It is therefore reasonable to conclude that all these platinum complexes, of all the monophosphines and diphosphines examined and regardless of the carboxylates used, are mononuclear in structure with the carboxylates in a monodentate state.

In an attempt to explain why the complexes opt for a mononuclear structure with monodentate acetate while the parent $[Pt(O_2CMe)_2]$ and its derivative $[Pt_4(en)_4(\mu\text{-}O_2CMe)_4]^{4+}$ adopt a tetranuclear framework *i.e.* $[Pt_4(\mu\text{-}O_2CMe)_8]$ based on an unusual octahedral geometry for Pt^{II} with bridging acetates (and chelating en) and Pt–Pt bonds, we have carried out a series of MO calculations using the Fenske–Hall method. For $[Pt_4(\mu\text{-}O_2CMe)_8]$ the molecule is aligned such that the Pt_4 core is approximately in the *xy* plane, and the Pt–Pt bonds are approximately parallel to either the *x* or *y* axis.

The distorted pseudo-octahedral co-ordination of the platinum atoms implies that their d orbitals are roughly split into 't_{2g}' (d_{xy}, d_{xz} and d_{yz}) and 'e_g' ($d_{x^2-y^2}$ and d_{z^2}) sets. The character of the molecular orbitals reveals a significant amount of mixing among the 't_{2g}' orbitals, which also mix a little with the 'e_g' orbitals, possibly to avoid net antibonding Pt–Pt π interactions between filled orbitals. Nevertheless, the calculated electronic populations of the atomic orbitals suggest that the

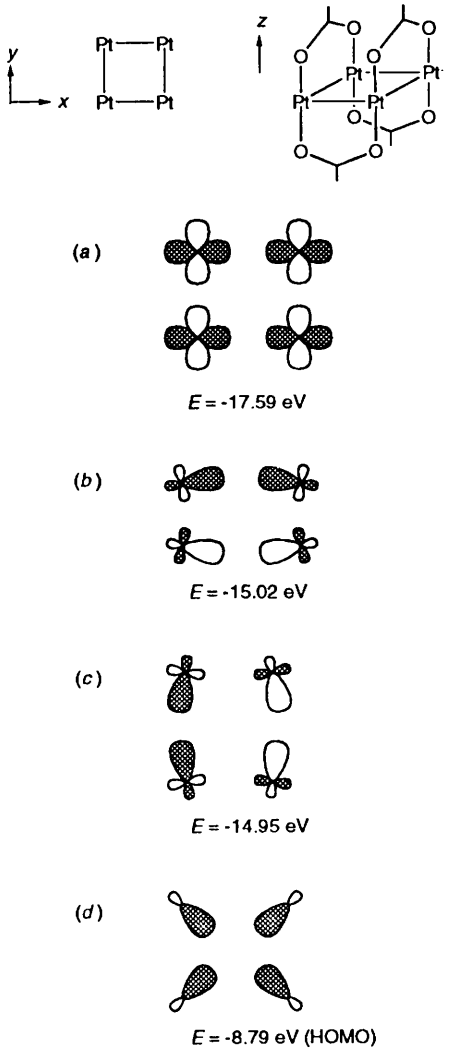

Fig. 4 Schematic representation of the four molecular orbitals describing Pt–Pt interactions in $[Pt_4(\mu\text{-}O_2CMe)_8]$ and the orbital energies

't_{2g}' orbitals are completely filled (Table 2), accounting for six electrons per Pt atom; there are thus two electrons per Pt left. Since the bonds in the *z*-direction are stronger (*i.e.* the Pt–O distances are shorter), the d_{z^2} orbitals are pushed higher in energy relative to the $d_{x^2-y^2}$ orbitals. Note that the latter are directed at neighbouring Pt atoms.

There are four molecular orbitals that describe Pt–Pt bonding. Three involve the $d_{x^2-y^2}$ orbitals, while in the fourth, contributions to bonding arise from d_{z^2} (the $x^2 + y^2$ component), d_{xy} (through π-bonding), s, p_x and p_y* (Fig. 4). Note that two of the $d_{x^2-y^2}$ combinations also include some d_{xy}, s, p_x and p_y contributions, so as to minimize Pt–Pt σ-antibonding interactions. One of the $d_{x^2-y^2}$ combinations (which is completely Pt–Pt antibonding) is unoccupied. The Pt–Pt overlap populations are 0.237, 0.234, 0.233 and 0.239, suggesting significant metal–metal bonding character.

Dividing the eight bonding electrons among the four 'bonds', each bond can formally be assigned two electrons. Thus, each Pt atom 'receives' four electrons as a result of metal–metal

* In the fourth orbital, there is some d_{xz} contribution which does not appear to serve any purpose other than the t_{2g} mixing mentioned earlier. The designation of this fourth MO as Pt–Pt bonding could be a subject of some controversy. However, we think it is justified, in view of the sizeable Pt–Pt overlap populations involving d_{z^2}, s and p orbitals. In support of this argument, the breakdown of contributions to the Pt(1)–Pt(2) overlap populations is given as SUP 57136. This bond is parallel to the *x* axis.

Table 2 Mulliken populations of atomic orbitals on one Pt atom in $[Pt_4(\mu\text{-}O_2CMe)_8]$

Orbital	Population	Orbital	Population
d_{z^2}	1.043	s	0.530
$d_{x^2-y^2}$	1.248	p_x	0.290
d_{xy}	1.985	p_y	0.279
d_{xz}	1.971	p_z	0.228
d_{yz}	1.966		

bonding. Adding the eight electrons per Pt from the acetate ligands, each Pt can be assigned 18 electrons.

Focus is next placed on the square-planar geometry of the present complexes. It is generally acknowledged that this planar co-ordination geometry is favoured for d^8 metal complexes, resulting in a total of 16 electrons at the metal centre. While the present complexes $[Pt_4(\mu\text{-}O_2CMe)_8]$ and $[Pt_4(en)_4(\mu\text{-}O_2CMe)_4]^{4+}$ all possess Pt^{II} and carboxylate ligands, the last two are octahedral, have 18 electrons per Pt atom and Pt–Pt bonds. The question is, why is this so? {especially since the pendant oxygen atoms in $[Pt(O_2CMe)_2(L\text{–}L)]$ are nucleophilic, *i.e.* their lone-pair orbitals constitute the two highest-occupied MOs}. To paraphrase the question, what is different when phosphine ligands are introduced?

First, it is important to realize that nitrogen and oxygen donors are more electronegative and less polarizable, hence comparatively little σ-electron density is transferred to Pt. This is especially true for carboxylate ligands, where the formal negative charge causes the platinum orbital energies to increase, thus reducing their capacity to accept electron density. A corollary of this effect is that the electronic population of the platinum orbitals involved in σ-bonding is relatively low, and Pt becomes quite positively charged (Table 3). In contrast, phosphines donate a substantial amount of σ-electron density.

A second important factor is the ability of phosphine to accept electron density from Pt into its empty d orbitals; acetate and en (which do not have valence d orbitals) completely lack this capability. Owing to such π-bonding, the population of the filled 'non-bonding' platinum d orbitals decreases significantly. Such a decrease is not observed with nitrogen and oxygen donors (Table 4).

In the case of $[Pt_4(\mu\text{-}O_2CMe)_8]$ and its en derivative, formation of the tetrameric structure alleviates the problem of high positive charge and low σ-electron density. It can be observed from Tables 3 and 4 that in the en complex the charge on Pt decreases significantly and the σ-electron density (in the $d_{x^2-y^2}$, d_{z^2}, s and p orbitals) increases on forming the tetramer.* Reference can also be made to the 18-electron rule, which is based on the ideal of 'spherical' distribution of electron density about the metal centre: formation of the tetramers with concomitant increase in σ-electron density reduces the disparity between the populations of the platinum σ and non-bonding orbitals (as mentioned above, the occupancy of the latter is high because of lack of π back donation).

Another possible electronic factor is that the propensity of phosphine to π bond probably militates against the mixing that was found to stabilize the octahedral environment and Pt–Pt bonding in $[Pt_4(\mu\text{-}O_2CMe)_8]$. It should also be noted that phosphine ligands are bulky, and there may be steric problems in incorporating them into a structure like that of the en compound.

As to the question of why platinum(II) acetate does not form a dimeric structure like Rh^{II} in $[Rh_2(O_2CMe)_4]$, the difference lies in the d^7 state for Rh^{II} and for d^8 for Pt^{II}: the metal orbitals that are directed at each other d_{z^2} if the metal–oxygen bonds are parallel to the *xy* plane) are half filled for Rh^{II} but completely filled for Pt^{II}. Platinum is probably too large to tolerate the net repulsive interaction between two filled orbitals. Another possible dimeric structure involves two bridging and two chelating acetates, with no Pt–Pt bonds. Such a structure is probably unstable, first because of the above-mentioned problem with the platinum atomic charge and orbital occupancy, and secondly since the lone pairs on oxygen occupy 'sp^2' orbitals in the same plane as that of the carboxylate group the orientation of the lone pairs on acetate incurs inefficient overlap (Fig. 5).

As a model of what might happen if Pt is replaced by Pd, calculations were also done on $[Pd(O_2CMe)_2(dppm)]$ {constructed from $[Pt(O_2CCF_3)_2(dppm)]$, with bond lengths adjusted accordingly}, and the results were compared to those of $[Pt(O_2CMe)_2(dppm)]$. It was found that the Pd atom is less positively charged (+0.184 compared to +0.267) and the phosphorus atoms more positively charged (average +0.68 compared to +0.63). This may be attributed to the higher electronegativity of palladium. The movement of electron density from phosphorus to palladium as a result of σ-electron deficiency associated with having carboxylate ligands may explain the decomposition of $[Pd(O_2CMe)_2(PR_3)_2]$, in which one phosphine is oxidized and Pd undergoes a two-electron reduction, as reported by Jutand and co-workers.[5]

* All the acetates in $[Pt_4(\mu\text{-}O_2CMe)_8]$ are bridging: we did not think it appropriate to do a calculation on a single Pt with four monodentate acetates. The effect is the same, as can be seen from the platinum charge in $[Pt(O_2CMe)_2]$ and $[Pt_4(\mu\text{-}O_2CMe)_8]$.

Table 3 Calculated Mulliken charges on Pt^{II} in various acetate complexes

Compound	Charge
$[Pt(O_2CMe)_2(dppf)]$	+0.328
$[Pt(O_2CCF_3)_2(dppm)]$	+0.217
$[Pt(O_2CMe)_2(dppm)]$	+0.267
$[Pt(O_2CMe)_2(en)]^a$	+0.513
$[Pt(O_2CMe)_2(en)]^b$	+0.591
$[Pt(O_2CMe)_2]^c$	+0.806
$[Pt_4(\mu\text{-}O_2CMe)_4(en)_4]^{4+}$	+0.310
$[Pt_4(\mu\text{-}O_2CMe)_8]$	+0.470

[a] Square planar; 'cut-and-paste' from $[Pt(O_2CMe)_2(dppf)]$ and tetramer. [b] Based on structure of tetramer.[17] [c] Based on structure of $[Pt(O_2CMe)_2(dppf)]$ (this work).

Table 4 Electronic populations of platinum orbitals in $[Pt(O_2CMe)_2(dppf)]$, square-planar $[Pt(O_2CMe)_2(en)]$ and $[Pt_4(en)_4(\mu\text{-}O_2CMe)_4]^{4+}$

	Population		
Orbital	dppf complex	en complex	Tetrameric complex[a]
d_{z^2}	1.863	1.873	1.236
$d_{x^2-y^2}$	1.154	0.810	1.300
d_{xy}	1.698	1.983	1.986
d_{xz}	1.823	1.996	1.742[b]
d_{yz}	1.835	1.996	1.983
s	0.601	0.485	0.548
p_x	0.361	0.185	0.322
p_y	0.360	0.185	0.325
p_z	−0.024	−0.024	0.249

[a] One Pt atom. [b] Due to mixing (distorted octahedron).

Experimental

General

All manipulations were routinely carried out under a dry argon atmosphere using freshly distilled solvents. The instruments used have been previously reported.[20] Elemental analyses were performed by the Microanalytical Laboratory in the Chemistry Department in the National University of Singapore.

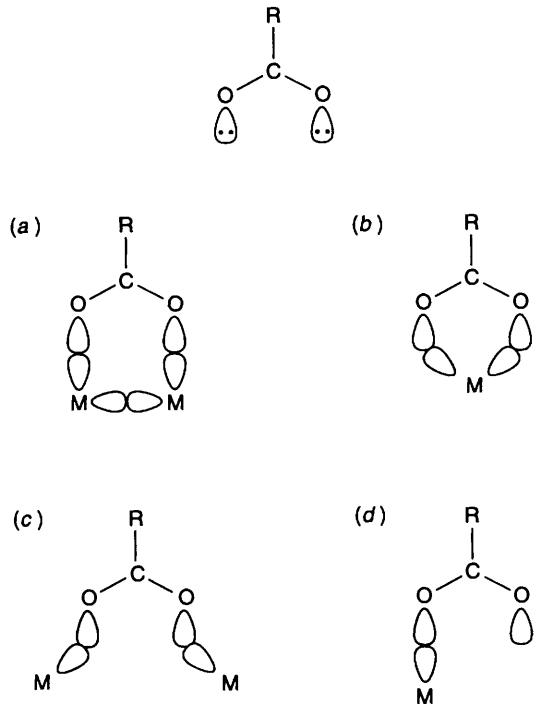

Fig. 5 Orientation of the lone-pair orbitals (*syn-syn*) in carboxylate ligands and a qualitative assessment of metal–oxygen overlap in various co-ordination modes: (*a*) bridging a M–M bond (good); (*b*) chelation (inefficient); (*c*) bridging, but without M–M bond (inefficient); (*d*) monodentate (good but unco-ordinated oxygen is nucleophilic)

Molecular-weight measurements were carried out by Galbraith Laboratories, Knoxville, TN, using vapour-pressure osmometry with a Knaüer-Dampfdruck osmometer. Infrared spectra were recorded on samples prepared in KBr discs, NMR spectra in $CDCl_3$ solutions on Brüker AMX500 (500 MHz for ^1H and 202.46 MHz for ^{31}P) or AC300F spectrometers (199.96 and 121.39 MHz respectively). The ^1H and ^{31}P spectra were referenced to $SiMe_4$ and 85% H_3PO_4 respectively.

Syntheses

[Pt(O$_2$CMe)$_2$(dppf)]. Solid $Ag(O_2CMe)$ (0.109 g, 0.64 mmol) was added to an orange-yellow solution of [$PtCl_2$(dppf)] (0.229 g, 0.28 mmol) in CH_2Cl_2 (*ca.* 60 cm^3). The resultant mixture was stirred, shielded from direct light, for *ca.* 20 h and filtered through a column of Celite to obtain a yellow solution. The filtrate was then evaporated *in vacuo* to give a dirty yellow-orange residue, which was redissolved in CH_2Cl_2 and filtered again through Celite to remove any residual silver particles. The filtrate was concentrated and hexane added to induce crystallization. Any silver metal formed during crystallization was removed by Celite filtration. Orange-yellow crystalline [$Pt(O_2CMe)_2$(dppf)] was obtained (0.167 g, 69%) (Found: C, 51.9; H, 3.9; Fe, 6.1; P, 6.9; Pt, 22.0. $C_{38}H_{36}FeO_5P_2Pt$ requires C, 51.5; H, 4.1; Fe, 6.3; P, 7.0; Pt, 22.0%); $\tilde{\nu}_{max}/cm^{-1}(CO_2^-)$ 1625s, 1595s (sh), 1366s and 1308s; δ_H 1.93 (6 H, s, CH_3), 4.39 (4 H, s, C_5H_4), 4.40 (4 H, s, C_5H_4), 7.35–7.49 (12 H, m, Ph) and 7.82–7.89 (8 H, m, Ph); δ_P 5.09 [J(PtP) 3948 Hz].

[Pt(O$_2$CPh)$_2$(PPh$_3$)$_2$]. A solution of [$PtCl_2(PPh_3)_2$] (0.155 g, 0.20 mmol) and $Ag(O_2CPh)$ (0.095 g, 0.41 mmol) in CH_2Cl_2 (*ca.* 45 cm^3) was stirred, shielded from direct light, at r.t. for *ca.* 18 h. The beige suspension was filtered through a column of Celite to obtain a colourless solution. The solvent was then removed *in vacuo*, CH_2Cl_2 introduced to dissolve the greyish white residue and the solution filtered through Celite to remove any residual silver particles. The CH_2Cl_2 filtrate was concentrated and hexane added to give upon standing an off-white crystalline solid of [$Pt(O_2CPh)_2(PPh_3)_2$]·0.5CH_2Cl_2 (0.152 g, 81%) [Found: C, 59.45; H, 3.9; Cl, 5.8; P, 7.4; Pt, 22.65%; M 972 ($CHCl_3$). $C_{50.5}H_{41}ClO_4P_2Pt$ requires C, 60.4; H, 4.1; Cl, 3.5; P, 6.2; Pt, 19.4%; M 962]; $\tilde{\nu}_{max}/cm^{-1}(CO_2^-)$ 1639m, 1616m, 1575m, 1342s (br) and 1326s (sh); δ_H 5.29 (1 H, s, CH_2Cl_2), 6.97–7.02 (4 H, m, Ph), 7.10–7.17 (12 H, m, Ph), 7.23–7.28 (8 H, m, Ph), 7.39–7.42 (4 H, m, Ph) and 7.63–7.69 (12 H, m, Ph); δ_P 6.55 [J(PtP) 3838 Hz].

[Pt(O$_2$CMe)$_2$(PPh$_3$)$_2$]. A similar reaction between [$PtCl_2(PPh_3)_2$] (0.260 g, 0.33 mmol) and $Ag(O_2CMe)$ (0.120 g, 0.72 mmol) in CH_2Cl_2 (80 cm^3) gave [$Pt(O_2CMe)_2(PPh_3)_2$] (0.193 g, 72%) as an off-white microcrystalline solid (Found: C, 56.5; H, 4.2; P, 7.2; Pt, 23.1. $C_{40}H_{36}O_4P_2Pt$ requires C, 57.35; H, 4.3; P, 7.4; Pt, 23.3%); $\tilde{\nu}_{max}/cm^{-1}$ (CO_2^-) 1634s (br), 1597m (sh), 1364s (br), 1310 and 1302s; δ_H 1.35 (6 H, s, CH_3), 7.17–7.22 (12 H, m, Ph), 7.30–7.35 (6 H, m, Ph) and 7.54–7.61 (12 H, m, Ph); δ_P 5.13 [J(PtP) 3826 Hz].

[Pt(O$_2$CCF$_3$)$_2$(PPh$_3$)$_2$]. A similar reaction between [$PtCl_2(PPh_3)_2$] (0.150 g, 0.19 mmol) and $Ag(O_2CCF_3)$ (0.092 g, 0.42 mmol) in CH_2Cl_2 (40 cm^3) gave [$Pt(O_2CCF_3)_2(PPh_3)_2$] (0.067 g, 37%) as an off-white microcrystalline solid (Found: C, 50.6; H, 3.1; F, 11.7; P, 7.0; Pt, 19.4. $C_{40}H_{36}F_6O_4P_2Pt$ requires C, 50.8; H, 3.2; F, 12.05; P, 6.55; Pt, 20.6%); $\tilde{\nu}_{max}/cm^{-1}(CO_2^-)$ 1727s, 1700s and 1401m; δ_H 7.19–7.25 (12 H, m, Ph), 7.35–7.40 (6 H, m, Ph) and 7.56–7.57 (12 H, m, Ph); δ_P 4.38 [J(PtP) 3933 Hz].

[Pt(O$_2$CPr^i)$_2$(PPh$_3$)$_2$]. A similar reaction between [$PtCl_2(PPh_3)_2$] (0.106 g, 0.13 mmol) and $Ag(O_2CPr^i)$ (0.085 g, 0.47 mmol) in CH_2Cl_2 (*ca.* 35 cm^3) gave [$Pt(O_2CPr^i)_2(PPh_3)_2$]·0.5CH_2Cl_2 (0.080 g, 69%) as an off-white microcrystalline solid (Found: C, 54.9; H, 4.1; Cl, 5.3; P, 6.3; Pt, 20.8. $C_{42.5}H_{41}ClO_4P_2Pt$ requires C, 55.8; H, 4.5; Cl, 3.9; P, 6.8; Pt, 21.3%); $\tilde{\nu}_{max}/cm^{-1}(CO_2^-)$ 1627s (br), 1373m and 1341m; δ_H 0.59 [6 H, t, $J(H_aH_b)$ 7.5, CH_3], 1.63 [4 H, q, $J(H_aH_b)$, 7.5 CH_2], 5.30 (1 H, s, CH_2Cl_2), 7.16–7.21 (12 H, m, Ph), 7.29–7.34 (6 H, m, Ph) and 7.55–7.61 (12 H, m, Ph); δ_H 5.79 [J(PtP) 3818 Hz].

[Pt(O$_2$CMe)$_2$(dppm)]. A similar reaction between [$PtCl_2$(dppm)] (0.139 g, 0.21 mmol) and $Ag(O_2CMe)$ (0.081 g, 0.48 mmol) in CH_2Cl_2 (*ca.* 50 cm^3) gave [$Pt(O_2CMe)_2$(dppm)] (0.085 g, 57%) as an off-white microcrystalline solid (Found: C, 49.5; H, 4.0; P, 7.7; Pt, 32.9. $C_{29}H_{28}O_4P_2Pt$ requires C, 49.9; H, 4.05; P, 8.9; Pt, 28.0%); $\tilde{\nu}_{max}/cm^{-1}(CO_2^-)$ 1619s (br), 1592(sh), 1366s and 1309s; δ_H 1.96 (6 H, s, CH_3), 4.18 [t, J(PH) 9.9 Hz, CH_2P], 7.37–7.49 (12 H, m, Ph) and 7.76–7.83 (8 H, m, Ph); δ_P −68.60 [J(PtP) 3463 Hz].

[Pt(O$_2$CCF$_3$)$_2$(dppm)]. A similar reaction between [$PtCl_2$(dppm)] (0.145 g, 0.22 mmol) and $Ag(O_2CCF_3)$ (0.107 g, 0.48 mmol) in CH_2Cl_2 (*ca.* 40 cm^3) gave [$Pt(O_2CCF_3)_2$(dppm)] (0.100 g, 56%) as colourless crystals (Found: C, 43.5; H, 2.6; F, 11.5; P, 7.6; Pt, 23.0. $C_{29}H_{22}F_6O_4P_2Pt$ requires C, 43.2; H, 2.75; F, 14.15; P, 7.7; Pt, 24.2%); $\tilde{\nu}_{max}/cm^{-1}(CO_2^-)$ 1713s (sh), 1698s (br) and 1406m; δ_H 4.37 [2 H, t, J(PH) 10.8, CH_2P], 7.42–7.60 (12 H, m, Ph) and 7.77–7.84 (8 H, m, Ph); δ_P −66.25 [J(PtP) 3404 Hz].

[Pt(O$_2$CPr^i)$_2$(dppm)]. A similar reaction between [$PtCl_2$(dppm)] (0.210 g, 0.32 mmol) and $Ag(O_2CPr^i)$ (0.134 g, 0.74 mmol) in CH_2Cl_2 (*ca.* 50 cm^3) gave [$Pt(O_2CPr^i)_2$(dppm)] (0.151 g, 65%) as colourless crystals (Found: C, 51.1; H, 4.2; P, 8.4. $C_{31}H_{32}O_4P_2Pt$ requires C, 51.3; H, 4.3; P, 8.5%); $\tilde{\nu}_{max}/cm^{-1}(CO_2^-)$ 1616vs, 1373m and 1347m; δ_H 0.89 [6 H, t, $J(H_aH_b)$ 7.60, CH_3], 2.22 [4 H, q, $J(H_aH_b)$ 7.60, CH_2CO_2], 4.17 [2 H, tt, J(PH) 10.0, J(PtH) 74.3, CH_2P], 7.35–7.47 (12 H, m, Ph) and 7.80–7.87 (8 H, m, Ph); δ_P −66.21 [J(PtP) 3449 Hz].

[Pt(O$_2$CPh)$_2$(dppm)]. A similar reaction between [$PtCl_2$(dppm)] (0.186 g, 0.28 mmol) and $Ag(O_2CPh)$ (0.149 g, 0.65

Table 5 Crystallographic data and refinement details*

	$[Pt(O_2CMe)_2(dppf)]\cdot H_2O$	$[Pt(O_2CPh)_2(dppf)]\cdot CH_2Cl_2$	$[Pt(O_2CCF_3)_2(dppm)]$
M	885.5	1076.6	805.50
Crystal system	Monoclinic	Triclinic	Monoclinic
Space group	$P2_1/c$ (no. 14)	$P\bar{1}$ (no. 2)	$P2_1/n$
a/Å	18.915(1)	10.150(1)	10.486(1)
b/Å	10.052(1)	14.187(1)	13.673(1)
c/Å	18.609(1)	17.779(2)	20.991(6)
α/°	—	70.18(1)	—
β/°	99.00(1)	90.00(1)	90.00(3)
γ/°	—	69.04(1)	—
U/Å^3	3495(2)	2227.4(11)	3009.59(14)
Z	4	2	4
$F(000)$	1752	1068	1560
D_c/g cm^{-3}	1.683	1.605	1.778
R_{int} (from merging of equivalent reflections)	0.078	0.00	0.058
μ/mm^{-1}	4.548	3.698	4.84
Mean μr	0.728	0.74	—
Scan rate	36 frames, φ = 0–180°, $\Delta\varphi$ = 5°, 10 min per frame	60 frames, φ = 0–180°, $\Delta\varphi$ = 3°, 10 min per frame	50 frames, φ = −30 to 120°, $\Delta\varphi$ = 3°, 9 min per frame
hkl Ranges	−23 to 23, −12 to 12, 0–28	−12 to 12, −16 to 17, 0–22	−13 to 13, −17 to 0, −26 to 26
Observed data, n	5744 [$\|F_o\| \geqslant 5\sigma(\|F_o\|)$]	6637 [$\|F_o\| \geqslant 5\sigma(\|F_o\|)$]	4785 [$F > 4.0\sigma(F)$]
No. of variables, p	425	533	434
$10^6 g$ In weighting scheme w	2	5	100
R	0.028	0.056	0.041
R'	0.030	0.079	0.037
S	1.78	1.76	1.98
Residual extrema in final difference map/e Å^{-3}	+1.09 to −1.49	+1.10 to −1.84	+0.76 to −0.64

* Details in common: $R = \Sigma||F_o| - |F_c||/\Sigma|F_o|$; $R' = [\Sigma w(|F_o| - |F_c|)^2/\Sigma w|F_o|^2]^{\frac{1}{2}}$ (for O_2CMe and O_2CCF_3), $[\Sigma w^2(|F_o| - |F_c|)^2/\Sigma w^2|F_o|^2]^{\frac{1}{2}}$ (for O_2CPh); $S = [\Sigma w(|F_o| - |F_c|)^2/(n - p)]^{\frac{1}{2}}$; $w^{-1} = \sigma^2(F_o) + gF^2$.

mmol) in CH_2Cl_2 (*ca.* 50 cm^3) gave $[Pt(O_2CPh)_2(dppm)]$ (0.175 g, 74%) as an off-white crystalline solid (Found: C, 56.8; H, 3.9; P, 7.5; Pt, 25.8. $C_{39}H_{32}O_4P_2Pt$ requires C, 56.9; H, 3.9; P, 7.5; Pt, 23.7%); $\tilde{\nu}_{max}$/cm^{-1}(CO_2^-) 1635m (sh), 1615s (br), 1574m, 1553m and 1333s (br); δ_H 4.29 [t, J(PH) 10.1, CH_2P], 7.24–7.45 (18 H, m, Ph) and 7.89–7.99 (12 H, m, Ph); δ_P −67.35 [J(PtP) 3437 Hz].

$[Pt(O_2CCF_3)_2(dppf)]$. A similar reaction between $[PtCl_2(dppf)]$ (0.127 g, 0.15 mmol) and $Ag(O_2CCF_3)$ (0.082 g, 0.37 mmol) in CH_2Cl_2 (*ca.* 35 cm^3) gave $[Pt(O_2CCF_3)_2(dppf)]$ (0.081 g, 54%) as an orange crystalline solid (Found: C, 46.4; H, 2.9; F, 6.0; Fe, 7.8; P, 5.3; Pt, 22.2. $C_{38}H_{28}F_6FeO_4P_2Pt$ requires C, 46.8; H, 2.9; F, 11.8; Fe, 5.7; P, 6.35; Pt, 20.0%); $\tilde{\nu}_{max}$/cm^{-1} (CO_2^-) 1725s, 1702s and 1397s; δ_H 4.43 [4 H, d, J(HH) 16, C_5H_4], 4.48 (4 H, s, C_5H_4), 7.37–7.42 (8 H, m, Ph), 7.49–7.54 (4 H, m, Ph) and 7.74–7.81 (8 H, m, Ph); δ_P 5.74 [J(PtP) 4064 Hz].

$[Pt(O_2CPr^i)_2(dppf)]$. A similar reaction between $[PtCl_2(dppf)]$ (0.137 g, 0.17 mmol) and $Ag(O_2CPr^i)$ (0.066 g, 0.36 mmol) in CH_2Cl_2 (*ca.* 35 cm^3) gave $[Pt(O_2CPr^i)_2(dppf)]$ (0.100 g, 60%) as orange crystals [Found: C, 53.1; H, 4.1; Fe, 5.6; P, 6.6; Pt, 26.8%; M 827 ($CHCl_3$); $C_{46}H_{38}FeO_4P_2Pt$ requires C, 53.6; H, 4.3; Fe, 6.2; P, 6.9; Pt, 21.8%; M 896]; $\tilde{\nu}_{max}$/cm^{-1}(CO_2^-) 1604s (br) and 1332s; δ_H 0.59 [6 H, t, $J(H_aH_b)$ 7.5, CH_3], 1.63 [4 H, q, $J(H_aH_b)$ 7.5, CH_2CO_2], 4.39 (8 H, s, C_5H_4), 4.38 (8 H, s, C_5H_4), 7.33–7.47 (12 H, m, Ph) and 7.82–7.88 (8 H, m, Ph); δ_P 5.68 [J(PtP) 3941 Hz].

$[Pt(O_2CPh)_2(dppf)]\cdot 0.5CH_2Cl_2$. A similar reaction between $[PtCl_2(dppf)]$ (0.250 g, 0.30 mmol) and $Ag(O_2CPh)$ (0.153 g, 0.67 mmol) in CH_2Cl_2 (*ca.* 80 cm^3) gave $[Pt(O_2CPh)_2(dppf)]$ (0.207 g, 73%) as orange crystals (Found: C, 56.5; H, 4.0; Fe, 5.2; P, 7.3; Pt, 17.85. $C_{48.5}H_{39}ClFeO_4P_2Pt$ requires C, 56.3; H, 3.8; Fe, 5.3; P, 6.0; Pt, 18.8%); $\tilde{\nu}_{max}$/cm^{-1}(CO_2^-) 1632s, 1356m and 1344s; δ_H 4.4 (br, 4 H, s, H_α of C_5H_4), 4.48 (br, 4 H, s, H_β of C_5H_4), 6.97–7.02 (4 H, Ph), 7.10–7.15 [2 H, t, J(HH) 7.2, Ph], 7.28–7.41 (16 H, m, Ph) and 7.89–7.95 (8 H, m, Ph); δ_P 6.69 [J(PtP) 3960 Hz].

Crystallography

Single crystals of $[Pt(O_2CMe)_2(dppf)]\cdot H_2O$ (orange-yellow prism, 0.25 × 0.30 × 0.40 mm), $[Pt(O_2CPh)_2(dppf)]\cdot CH_2Cl_2$ (yellow prism, 0.30 × 0.40 × 0.50 mm) and $[Pt(O_2CCF_3)_2(dppm)]$ (colourless prism, 0.08 × 0.12 × 0.28 mm) were grown from CH_2Cl_2–hexane mixtures.[3] Those suitable for X-ray diffraction were mounted on top of glass fibres. Intensity data were measured on a Rigaku RAXIS-IIC[31] imaging-plate diffractometer system powered at 50 kV and 90 mA with graphite-monochromatized Mo-Kα radiation (λ 0.710 73 Å) using the variable ω-scan technique. Two standard reflections were monitored after every 125 data measurements, showing only small random variations. The raw data were processed with the learnt-profile procedure,[32] and absorption corrections were applied by fitting a pseudo-ellipsoid to the ψ-scan data for selected strong reflections over a range of 2θ angles.[33] All the structures were solved with the Patterson superposition method and subsequent Fourier-difference syntheses. The CF_3 groups in $[Pt(O_2CCF_3)_2(dppm)]$ are disordered. For both dppf structures the final difference map contained residual extrema exceeding ± 1 e Å^{-3} in the neighbourhood of the heavy Pt atom. All the non-hydrogen atoms were refined anisotropically. Hydrogen atoms of the organic ligands were generated geometrically (C–H 0.95 Å), assigned appropriate isotropic thermal parameters, and allowed to ride on their parent carbon atoms. The phenyl groups on the phosphines were treated as rigid groups. The other non-hydrogen atoms were refined anisotropically, and the hydrogen atoms of the cyclopentadienyl groups were included in structure-factor calculations with assigned isotropic thermal parameters. All computations were performed with the SHELXTL-PC program package.[34] Analytical expressions of neutral-atom scattering factors were employed, and anomalous-dispersion corrections were incorporated.[35] Crystal data, data-collection parameters, and results of the analyses are listed in Table 5.

Atomic coordinates, thermal parameters and bond lengths and angles have been deposited at the Cambridge Crystallographic Data Centre (CCDC). See Instructions for Authors, *J. Chem. Soc., Dalton Trans.*, 1996, Issue 1. Any request to the

CCDC for this material should quote the full literature citation and the reference number 186/31.

Theoretical calculations

The models of the molecules used for the calculations are based on their crystal structures. Those of $[Pt_4(\mu\text{-}O_2CMe)_8]$ and $[Pt_4(en)_4(\mu\text{-}O_2CMe)_4]^{4+}$ were aligned such that the Pt_4 plane lies on the xy plane and the Pt–Pt bonds along the x and y axes. For $[Pt(O_2CMe)_2(L\text{–}L)]$ and related compounds all Pt–P and Pt–O bonds were aligned to be approximately parallel to either the x or the y axis. Where substitutions were made, *e.g.* $MeCO_2$ for CF_3CO_2 and Pd for Pt, the bond lengths were adjusted based on the covalent radii of atoms concerned.

Calculations were performed using the self-consistent Fenske–Hall approximate molecular orbital method.[36] The basis functions were obtained by fitting the results of Xα (Herman–Skillman)[37] calculations to Slater orbitals;[38] double-ζ functions were used for transition-metal d orbitals and main group p orbitals. As a common practice in Fenske–Hall calculations, the exponents of the platinum valence s and p orbitals were fixed at 2.4, and those of Pd at 2.2. An exponent of 1.2 was used for hydrogen. Mulliken population analyses[39] were employed to calculate atomic charges and overlap populations.

Acknowledgements

We acknowledge the National University of Singapore (NUS) (RP850030) and the Hong Kong Research Grants Council Earmarked Grant CUHK 311/94P for financial support and technical assistance from the Department of Chemistry, NUS. We thank Professor T. Ito of Tohoku University for supplying his crystallographic data on $[Pt_4(en)_4(\mu\text{-}O_2CMe)_4]^{4+}$ for our calculations and Y. P. Leong for assistance in the preparation of this manuscript. A. L. T. acknowledges a fellowship award from the National Science and Technology Board (NSTB), Singapore and the NSTB for the use of MSI Cerius2 software. P. M. N. L. thanks NUS for a scholarship award, and B.-M. W. thanks the Institute of Biophysics, Chinese Academy of Sciences, Beijing for sabbatical leave.

References

1 C. Oldham, in *Comprehensive Coordination Chemistry*, eds. G. Wilkinson, R. D. Gillard and J. A. McCleverty, Pergamon, Oxford, 1987, vol. 2, ch. 15.6, p. 435.
2 D. Lyons, G. Wilkinson, M. Thornton-Pett and M. B. Hursthouse, *J. Chem. Soc., Dalton Trans.*, 1984, 695.
3 C. J. Nyman, C. T. Wymore and G. Wilkinson, *J. Chem. Soc. A*, 1968, 561.
4 C. Eaborn, K. J. Odell and A. Pidcock, *J. Chem. Soc., Dalton Trans.*, 1979, 758; M. J. Broadhurst, J. M. Brown and R. A. John, *Angew. Chem., Int. Ed. Engl.*, 1983, **22**, 47.
5 C. Amatore, A. Jutand and M. A. M'Barki, *Organometallics*, 1992, **11**, 3009; C. Amatore, E. Carré, A. Jutand and M. A. M'Barki, *Organometallics*, 1995, **14**, 1818.
6 T. A. Stephenson, S. M. Morehouse, A. R. Powell, J. P. Heffer and G. Wilkinson, *J. Chem. Soc.*, 1965, 3632.
7 S. Cacchi and A. Arcadi, *J. Org. Chem.*, 1983, **48**, 4236; H. Iida, Y. Yuasa and C. Kibayashi, *J. Org. Chem.*, 1980, **45**, 2938; C. M. Andersson, J. Larsson and A. Hallberg, *J. Org. Chem.*, 1990, **52**, 5757.
8 R. F. Heck, *Acc. Chem. Res.*, 1979, **12**, 146; M. Kumada, *Pure Appl. Chem.*, 1980, **52**, 669; E. I. Negishi, *Acc. Chem. Res.*, 1982, **15**, 340; R. F. Heck, *Palladium Reagents in Organic Syntheses*, Academic Press, New York, 1985; J. K. Stille, *Angew. Chem. Int., Ed. Engl.*, 1986, **25**, 508.
9 P. M. N. Low and T. S. A. Hor, unpublished work.
10 T. A. Stephenson and G. Wilkinson, *J. Inorg. Nucl. Chem.*, 1967, **29**, 2122; T. R. Jack and J. Powell, *Can. J. Chem.*, 1975, **53**, 2558.
11 H. Yoshimoto and H. Itatani, *Bull. Chem. Soc. Jpn.*, 1973, **46**, 2490; J. A. Goodfellow, T. A. Stephenson and M. C. Cornock, *J. Chem. Soc., Dalton Trans.*, 1978, 1195; B. A. Patel, L.-C. Kao, N. A. Cortese, J. V. Minkiewicz and R. F. Heck, *J. Org. Chem.*, 1979, **44**, 918; *Dictionary of Inorganic Compounds*, eds. J. E. Macintyre, F. M. Daniel and V. M. Stirling, Chapman & Hall, London, 1992, vol. 2, p. 2421.
12 C. Bird, B. L. Booth, R. N. Haszeldine, G. R. H. Neuss, M. A. Smith and A. Flood, *J. Chem. Soc., Dalton Trans.*, 1982, 1109.
13 A. Dobson, S. D. Robinson and M. F. Uttley, *Inorg. Synth.*, 1977, **17**, 124; J. Kuyper, *Inorg. Chem.*, 1979, **18**, 1484.
14 *Dictionary of Inorganic Compounds*, eds. J. E. Macintyre, F. M. Daniel and V. M. Stirling, Chapman & Hall, London, 1992, vol. 2, p. 2421.
15 D. M. Blake, S. Shields and L. Wyman, *Inorg. Chem.*, 1974, **13**, 1595.
16 M. A. A. F. de C. T. Carrondo and A. C. Skapski, *J. Chem. Soc., Chem. Commun.*, 1976, 410; *Acta Crystallogr., Sect. B*, 1978, **34**, 1857, 3576.
17 T. Yamaguchi, T. Ueno and T. Ito, *Inorg. Chem.*, 1993, **32**, 4996.
18 T. Hayashi, M. Konishi, Y. Kobori, M. Kumada, T. Higuchi and K. Hirotsu, *J. Am. Chem. Soc.*, 1984, **106**, 158.
19 T. Yanagi, T. Ohe, N. Miyaura and A. Suzuki, *Bull. Chem. Soc. Jpn.*, 1989, **62**, 3892.
20 S. P. Neo, Z.-Y. Zhou, T. C. W. Mak and T. S. A. Hor, *J. Chem. Soc., Dalton Trans.*, 1994, 3451.
21 T. S. A. Hor, S. P. Neo, C. S. Tan, T. C. W. Mak, K. W. P. Leung and R. J. Wang, *Inorg. Chem.*, 1992, **31**, 4510.
22 G. Douglas, L. Manojlovic-Muir, K. W. Muir, M. C. Jennings, B. R. Lloyd, M. Rashidi, G. Schoettel and R. J. Puddephatt, *Organometallics*, 1991, **10**, 3927.
23 W. Beck, K. Schorpp and K. H. Stetter, *Z. Naturforsch., Teil B*, 1971, **26**, 684.
24 G. K. Anderson and G. J. Lumetta, *Inorg. Chem.*, 1987, **26**, 1291.
25 N. Hadj-Bagheri and R. J. Puddephatt, *Inorg. Chem.*, 1989, **28**, 2384; *J. Chem. Soc., Chem. Commun.*, 1987, 1269; L. Manojlovic-Muir, K. W. Muir, M. C. Grossel, M. P. Brown, C. D. Nelson, A. Yavari, E. Kallas, R. P. Moulding and K. R. Seddon, *J. Chem. Soc., Dalton Trans.*, 1986, 1955.
26 Z.-G. Fang, P. M. N. Low, S.-C. Ng and T. S. A. Hor, *J. Organomet. Chem.*, 1994, **483**, 17.
27 C. K. Johnson, ORTEP, Report ORNL-5138, Oak Ridge National Laboratory, Oak Ridge TN, 1976.
28 A. Sacco, G. Vasapollo, C. F. Nobile, A. Piergiovanni, M. A. Pellinghelli and M. Lanfranchi, *J. Organomet. Chem.*, 1988, **356**, 397; G. Vasapollo, L. Toniolo, G. Cavinato, F. Bigoli, M. Lanfranchi and M. A. Pellinghelli, *J. Organomet. Chem.*, 1994, **481**, 173.
29 M. Zhou, Y. Xu, A.-M. Tan, P.-H. Leung, K. F. Mok, L.-L. Koh and T. S. A. Hor, *Inorg. Chem.*, 1995, **34**, 6425; A. L. Bandini, G. Banditelli, M. A. Cinellu, G. Sanna, G. Minghetti, F. Demartin and M. Manassero, *Inorg. Chem.*, 1989, **28**, 404; B. Longato, G. Pilloni, G. Valle and B. Corain, *Inorg. Chem.*, 1988, **27**, 956; G. Bandoli, G. Trovo, A. Dolmella and B. Longato, *Inorg. Chem.*, 1992, **31**, 45; B. S. Haggerty, C. E. Housecroft, A. L. Rheingold and B. A. M. Shaykh, *J. Chem. Soc., Dalton Trans.*, 1991, 2175.
30 K.-S. Gan and T. S. A. Hor, in *Ferrocene*, eds. A. Togni and T. Hayashi, VCH, Weinheim, 1995, ch. 1, p. 3.
31 M. Sato, M. Yamamoto, K. Imada, Y. Katsube, N. Tanaka and T. Higashi, *J. Appl. Crystallogr.*, 1992, **25**, 348.
32 R. Diamond, *Acta Crystallogr., Sect. A*, 1969, **25**, 43.
33 G. Kopfmann and R. Huber, *Acta Crystallogr., Sect. A*, 1968, **24**, 348.
34 G. Sheldrick, SHELXTL-PC, Program Package for X-Ray Crystal Structure Determination, Siemens Analytical Instruments, Inc., Karlsruhe, 1990.
35 *International Tables for X-ray Crystallography*, Kynoch Press, Birmingham, 1974, vol. 4, p. 55, 99, 149.
36 M. B. Hall and R. F. Fenske, *Inorg. Chem.*, 1972, **11**, 768.
37 F. Herman and S. Skillman, *Atomic Structure Calculations*, Prentice-Hall, Englewood Cliffs, NJ, 1963.
38 B. E. Bursten, J. R. Jensen and R. F. Fenske, *J. Chem. Phys.*, 1978, **68**, 3320.
39 R. S. Mulliken, *J. Chem. Phys.*, 1955, **23**, 1841.

Received 15*th December* 1995; *Paper* 5/08163G